Effect of Phenethylammonium Thiocyanate Additive in Tin Perovskite for Efficient and Stable Pb-free Perovskite Solar Cells

Dhruba B. Khadka[1], Yasuhiro Shirai[1], Masatoshi Yanagida[1] and Kenjiro Miyano[1]

[1] Photovoltaics Materials Group, Global Research Center for Environment and Energy based on Nanomaterials Science (GREEN), National Institute for Materials Science (NIMS), 1-1 Namiki, Tsukuba, Ibaraki 305-0044, Japan.

Abstract— The phenethylammonium thiocyanate (PEASCN) was introduced into the $FASnI_3$ perovskite film as a pseudohalide functional additive. This results in the suppression of Sn-oxidation and compact and larger grain film with better crystallinity. The device with PEASCN additive improved the power conversion efficiency (PCE) from 4.52% (control) to 9.65% (PEASCN). The device analysis revealed that the PEASCN additive has improved the optoelectronic properties coupled with a higher diffusion potential and passivation of defect densities in the Sn-PSCs. This report suggests that the pseudohalide-based functional additive is propitious for film growth, modification of surface chemistry, and defects at interface and bulk.

Keywords—Tin perovskite, Pseudohalide, tin oxidation, additive, stability, defect density.

I. Introduction

Tin and Bismuth based-perovskite solar cells (Sn/Bi-PSC) are alternative to lead-based halide perovskite devices to solve the toxicity issue of lead.[1]–[4] The intrinsic instability of Sn-HaP due to the facile oxidation of Sn^{2+} to Sn^{4+} leads to the formation of tin vacancy and metal-like behavior that deteriorates the device performance.[5] Several approaches have been introduced that passivate the catastrophic effects in Sn-HaP film quality by structural regulation and additive engineering which results in improving the device performance and its stability.[6] A number of additives have been used as reducing agents to inhibit the oxidation and facilitate the formation of a pinhole-free uniform film.[7] The A-site alloying in $FASnI_3$ crystal lattice has demonstrated improvement in the device performance and stability by regulating 3D structure.[8], [9] Besides this, a thin 2D layer was formed on the top of the 3D layer by post-treatment.[10], [11] Moreover, additives with pseudohalide functional derivatives increase the device performance of HaPSCs and stability coupled with the hydrophobicity and optoelectronic quality of HaP film.[12], [13] The additive with N-, S-, and O-based electron donors conjugate with tin halides by donating a lone pair electron to the divalent tin resulting increase in covalency.[14] Noting that the pseudohalide derivatives is beneficial for stabilizing the halide bonding.[15]–[17]

In this work, the bulky organic cation pseudohalide PEASCN was added in the $FASnI_3$ precursor to control the extent of tin oxidation and film growth. The pseudohalide of the PEASCN additive effectively improves the film quality and optoelectronic properties. The PCE enhanced from 4.52% for pristine to 9.65% for PEASCN added device with better stability. We have explored the characteristics insight into the effect of PEASCN additive by analysing the growth, optophysical, optoelectronic properties.[18] This report has discussed the additive approach to pave the way for addressing the oxidation and instability issue of Sn-HaPSCs.

II. Experimental

A. Device fabrication

For the fabrication of $FASnI_3$; 0.8 M of FAI, SnI_2, and SnF_2 (0.08 M) and for PEASCN incorporated $FASnI_3$, PEASCN: FAI (x, 1-x); 0.8 M), SnI_2 (0.8 M), and SnF_2 (0.08 M) were dissolved in dimethyl sulfoxide (DMSO) solvent for one hour. The Sn-HaP precursor was deposited on the PEDOT:PSS (30 nm)/ITO substrate. These films were annealed on the hot plate at 60 ℃ for 3min and 100 ℃ for 10 min. Then, the device is completed depositing PCBM /BCP thin films were spun–coated on top of the Sn-HaP films. The detailed fabrication can be found in our earlier report.[18], [19] Finally, Ag (100 nm) was thermally evaporated and get device of ~0.26 cm^2 area.

B. Materials and device characterizations

The XRD results were collected using Rigaku Smart Lab, CuK_α radiation, λ=1.5405Å. The SEM images were obtained by a high-resolution scanning electron microscope (SEM) at 5 kV accelerating voltage (Hitachi, S-4800). XPS spectra were obtained using a Versa Probe II (ULVAC-PHI, Japan). The current density–voltage (*J-V*) curves were measured under 1 sun with an AM1.5G spectral filter (100 mW/cm^2) coupled with an MPPT system (Systemhouse Sunrise Corp.). capacitance spectra (*C–f*) were collected using an LCR meter (IM3536, Hioki) under dark.

III. Results and Discussion

Figure 1a shows a complete device with the structure of ITO/PEDOT:PSS/$FA_{1-x}PEASCN_xSnI_3$/PCBM/BCP/Ag. The device parameters with PEASCN additive are given in Fig. 1c and J-V curves (Fig. 1b). The device with PEASCN additive ($x \leq 0.08$) exhibited a PCE of ~9.65% (J_{SC}~ 22.16 $mAcm^{-2}$,

V_{OC}~ 0.667V, and FF= 65.3) with negligible hysteresis. It showed a significant improvement in PCE of 4.52% for control device. The device with PEASCN additive (Fig.1d) revealed superior device stability compared to the control device.

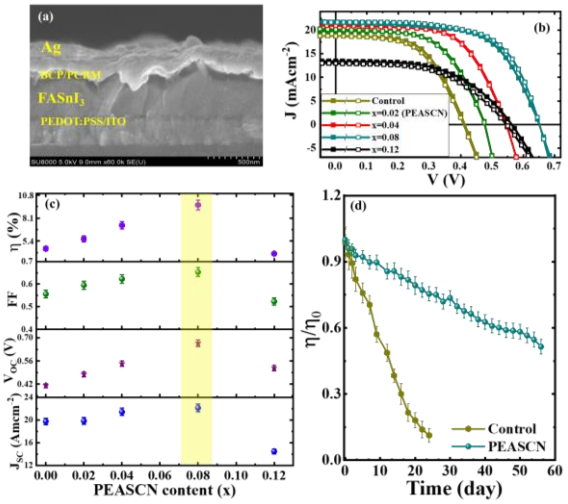

Fig. 1. Cross-sectional image of the device (a). The *J-V* curves of $FA_{1-x}PEASCN_xSnI_3$ devices (for x=0 - 0.12) (b). Device parameters with varying content of PEASCN (c). x=0.08 is optimal denoted as PEASCN hereafter. normalized efficiency with the stability of pristine and PEASCN incorporated devices (d).

The SEM images (Fig. 1a, b) shows a better film coverage and large grains for the film with PEASCN (x=0.08) compared to the control (x=0). It grows with highly oriented crystallographic planes of (100) and (200) for with PEASCN additive whereas the control film has with multiple crystal orientations i.e. (102), (122), (222), (213), etc. No 2D phase features were observed with PEASCN additive for x≤ 0.08.[18] This supports the improvement in device performance.

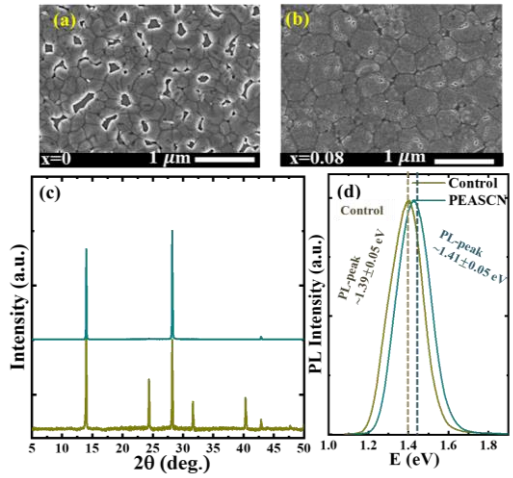

Fig. 2. SEM images (a,b), XRD patterns (c) and PL spectra (d) of the $FA_{1-x}PEASCN_xSnI_3$ films with contents (x=0, 0.08 (PEASCN)).

The Photoluminescence (PL) spectra of the corresponding films (Fig.2d) reveal a slight blueshift of characteristics peaks with the PEASCN additive. The characteristic PL peaks are centred at 1.40±0.02 eV for x=0 and 1.41±0.02 eV for x=0.08. This modifies the interface band alignment which increase the carrier transport.

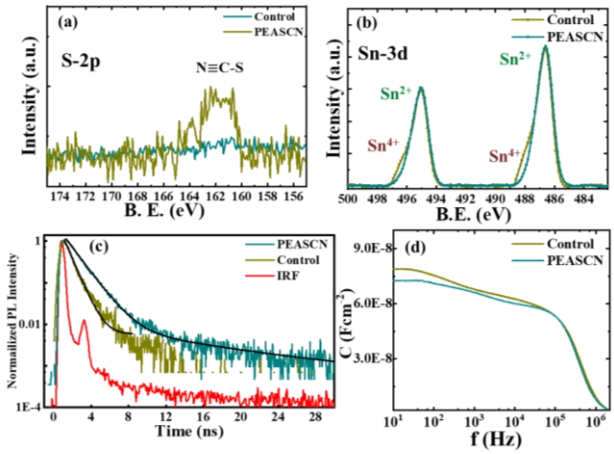

Fig. 3. XPS spectra (S-2p, Sn-3d) of the respective film (a,b). TRPL results of films (c). C-f spectra at room temperature (d).

To get insight into the effect of the PEASCN, the surface chemistry of $FASnI_3$ film was examined by X-ray photoelectron spectroscopy (XPS) measurement. Figure 3a shows the XPS core of S-2p indicating existence of SCN component on surface of film with PEASCN additive. The characteristics peak convoluted from the XPS spectra (Fig. 3b) at ~ 486.7 (495.2) eV and 487.3 (495.7) eV are assigned to the Sn^{2+} and Sn^{4+} species, respectively. We found that the control $FASnI_3$ film has a higher atomic percentage of Sn^{4+} compared with the PEASCN additive film. It corroborates that the PEASCN incorporation in the $FASnI_3$ lattice controls the extent of Sn^{2+} oxidation and hence ameliorates the film quality. This is concurrent with the device results. Figure 3c a depicts time-resolved PL (TRPL) characteristics of Sn-HaP film. It shows a longer carrier lifetime of 1.68 ns for the PEASCN added $FASnI_3$ film compared to the control film (0.64 ns). This implicates a lower defect density in the film with an additive that must be a consequence of the controlled growth of morphology with large grain and better crystallinity of film with additive.

Furthermore, the capacitance-frequency (*C-f*) response (Fig. 3d) for the control device shows a slightly larger value in the range of 1kHz to 50 kHz that arises from the absorber bulk. It is correlated with a higher defect density in the control Sn-HaP film which is prone to inferior device performance. The capacitance at a lower frequency has a lower value for the device with PEASCN additive. It is related to the reduction in ion or charge accumulation at the interfacial layer or electrode. This could result in improvement in device stability with PEASCN additive.

IV. Summary and Conclusions

In summary, we achieved Sn-PSCs of PEC ~9.65% using phenethylammonium thiocyanate (PEASCN) additive with improved stability. The Sn-HaP film with the PEASCN additive remarkably improved the film morphology and highly oriented crystal growth with control of Sn^{2+} to Sn^{4+} oxidation. The optophysical properties show that the $FASnI_3$ film with additive increases the carrier lifetime and reduces the band

offset. Our report implicates that the pseudohalide functional is beneficial for the improvement in optoelectronic quality of $FASnI_3$ film which collectively results in the performance and stability.

ACKNOWLEDGMENT

This work was supported by JST-Mirai Program Grant Number JPMJMI21E6, Japan.

REFERENCES

[1] G. Nasti and A. Abate, "Tin Halide Perovskite (ASnX3) Solar Cells: A Comprehensive Guide toward the Highest Power Conversion Efficiency," *Adv. Energy Mater.*, vol. 10, no. 13, p. 1902467, Apr. 2020, doi: 10.1002/aenm.201902467.

[2] D. B. Khadka, Y. Shirai, M. Yanagida, and K. Miyano, "Tailoring the film morphology and interface band offset of caesium bismuth iodide-based Pb-free perovskite solar cells," *J. Mater. Chem. C*, vol. 7, no. 27, pp. 8335–8343, 2019, doi: 10.1039/C9TC02181G.

[3] M. G. M. Pandian *et al.*, "Effect of solvent vapour annealing on bismuth triiodide film for photovoltaic applications and its optoelectronic properties," *J. Mater. Chem. C*, vol. 8, no. 35, pp. 12173–12180, 2020, doi: 10.1039/D0TC02455D.

[4] L. Liang and P. Gao, "Lead-Free Hybrid Perovskite Absorbers for Viable Application: Can We Eat the Cake and Have It too?," *Adv. Sci.*, vol. 5, no. 2, p. 1700331, Feb. 2018, doi: 10.1002/advs.201700331.

[5] T. Nakamura *et al.*, "Sn(IV)-free tin perovskite films realized by in situ Sn(0) nanoparticle treatment of the precursor solution," *Nat. Commun.*, vol. 11, no. 1, p. 3008, 2020, doi: 10.1038/s41467-020-16726-3.

[6] Y. Yan, T. Pullerits, K. Zheng, and Z. Liang, "Advancing Tin Halide Perovskites: Strategies toward the ASnX3 Paradigm for Efficient and Durable Optoelectronics," *ACS Energy Lett.*, vol. 5, no. 6, pp. 2052–2086, Jun. 2020, doi: 10.1021/acsenergylett.0c00577.

[7] C. Wang *et al.*, "Illumination Durability and High-Efficiency Sn-Based Perovskite Solar Cell under Coordinated Control of Phenylhydrazine and Halogen Ions," *Matter*, vol. 4, no. 2, 2021, doi: 10.1016/j.matt.2020.11.012.

[8] D. B. Khadka, Y. Shirai, M. Yanagida, and K. Miyano, "Attenuating the defect activities with a rubidium additive for efficient and stable Sn-based halide perovskite solar cells," *J. Mater. Chem. C*, vol. 8, no. 7, pp. 2307–2313, 2020, doi: 10.1039/C9TC06206H.

[9] X. Jiang *et al.*, "One-Step Synthesis of SnI2·(DMSO)x Adducts for High-Performance Tin Perovskite Solar Cells," *J. Am. Chem. Soc.*, vol. 143, no. 29, pp. 10970–10976, Jul. 2021, doi: 10.1021/jacs.1c03032.

[10] M. Liao *et al.*, "Efficient and Stable FASnI3 Perovskite Solar Cells with Effective Interface Modulation by Low-Dimensional Perovskite Layer," *ChemSusChem*, vol. 12, no. 22, pp. 5007–5014, Nov. 2019, doi: 10.1002/cssc.201902000.

[11] T. Wu *et al.*, "Efficient and Stable Tin Perovskite Solar Cells Enabled by Graded Heterostructure of Light-Absorbing Layer," *Sol. RRL*, vol. 4, no. 9, p. 2000240, Sep. 2020, doi: 10.1002/solr.202000240.

[12] Y. Numata, Y. Sanehira, R. Ishikawa, H. Shirai, and T. Miyasaka, "Thiocyanate Containing Two-Dimensional Cesium Lead Iodide Perovskite, Cs 2 PbI 2 (SCN) 2 : Characterization, Photovoltaic Application, and Degradation Mechanism," *ACS Appl. Mater. Interfaces*, vol. 10, no. 49, pp. 42363–42371, 2018, doi: 10.1021/acsami.8b15578.

[13] H. Kim, J. W. Lee, G. R. Han, S. K. Kim, and J. H. Oh, "Synergistic Effects of Cation and Anion in an Ionic Imidazolium Tetrafluoroborate Additive for Improving the Efficiency and Stability of Half-Mixed Pb-Sn Perovskite Solar Cells," *Adv. Funct. Mater.*, vol. 31, no. 11, p. 2008801, Mar. 2021, doi: 10.1002/adfm.202008801.

[14] X. Meng *et al.*, "Highly Stable and Efficient FASnI 3 -Based Perovskite Solar Cells by Introducing Hydrogen Bonding," *Adv. Mater.*, vol. 31, no. 42, p. 1903721, Oct. 2019, doi: 10.1002/adma.201903721.

[15] B. Yu *et al.*, "Efficient (>20%) and Stable All-Inorganic Cesium Lead Triiodide Solar Cell Enabled by Thiocyanate Molten Salts," *Angew. Chemie Int. Ed.*, vol. 60, no. 24, pp. 13436–13443, Jun. 2021, doi: 10.1002/anie.202102466.

[16] Y. Yu *et al.*, "Synergistic Effects of Lead Thiocyanate Additive and Solvent Annealing on the Performance of Wide-Bandgap Perovskite Solar Cells," *ACS Energy Lett.*, vol. 2, no. 5, pp. 1177–1182, May 2017, doi: 10.1021/acsenergylett.7b00278.

[17] M. Rameez, S. Shahbazi, P. Raghunath, M. C. Lin, C. H. Hung, and E. W.-G. Diau, "Development of Novel Mixed Halide/Superhalide Tin-Based Perovskites for Mesoscopic Carbon-Based Solar Cells," *J. Phys. Chem. Lett.*, vol. 11, no. 7, pp. 2443–2448, Apr. 2020, doi: 10.1021/acs.jpclett.0c00479.

[18] D. B. Khadka, Y. Shirai, M. Yanagida, and K. Miyano, "Pseudohalide Functional Additives in Tin Halide Perovskite for Efficient and Stable Pb-Free Perovskite Solar Cells," *ACS Appl. Energy Mater.*, vol. 4, no. 11, pp. 12819–12826, Nov. 2021, doi: 10.1021/acsaem.1c02496.

[19] D. B. Khadka, Y. Shirai, M. Yanagida, T. Masuda, and K. Miyano, "Enhancement in efficiency and optoelectronic quality of perovskite thin films annealed in MACl vapor," *Sustain. Energy Fuels*, vol. 1, no. 4, pp. 755–766, 2017, doi: 10.1039/C7SE00033B.